Emergent Spacetime Signatures from Minimal Quantum Circuits: Entanglement, Entropy, and Real-Hardware Evidence

A Multi-Experiment Study on IBM Quantum Hardware and Simulators

Ankitkumar Patel
Trium Designs Pvt Ltd

26 June 2025

Abstract

We present a multi-experiment study investigating emergent phenomena in quantum systems, exploring entropy signatures and bitstring distributions across various circuit architectures. Our work includes: (1) a 4-qubit circuit designed as a **minimal toy model for emergent gravitational and gauge structures** executed on real IBM Quantum hardware; (2) an 8-qubit linear chain with conditional evolution simulated noiselessly; and (3) a 9-qubit 2D grid experiment executed on real IBM Quantum hardware. By analyzing final bitstring distributions and entropy landscapes, we uncover signatures of entropy growth, gauge-gravity entanglement, and proto-holographic encoding, as well as the impact of circuit topology and real-world noise. Our results demonstrate that both small-scale and more complex quantum systems can reveal insights into emergent geometric and information-theoretic properties, laying groundwork for future investigations into quantum gravity analogies and complex quantum many-body dynamics.

1 Introduction

The idea that fundamental physical phenomena, including spacetime and its properties, may emerge from underlying quantum information structures, such as entanglement, is a central theme in modern theoretical physics [1, 2, 3]. While theoretical investigations into these "emergent" paradigms (e.g., ER=EPR, AdS/CFT, holographic error correction) continue to advance, experimental probes remain challenging. Recent progress in quantum computing, particularly with noisy intermediate-scale quantum (NISQ) devices, offers a unique opportunity to explore such concepts in controlled, albeit finite, quantum systems.

In this work, we present a comprehensive study across three distinct quantum circuit experiments, each designed to shed light on different facets of emergent behavior:

- A 4-qubit circuit specifically constructed and interpreted as a **minimal toy model for emergent bulk geometry**, with explicit qubit assignments for gravitational, gauge, and matter degrees of freedom, executed on real quantum hardware.
- An 8-qubit linear chain, simulated in a noiseless environment, to probe ideal entanglement spread and the formation of low-entropy states under conditional evolution.
- A 9-qubit 2D grid, executed on real IBM Quantum hardware, to investigate spatial correlations and the resilience of emergent patterns in a more complex topological "fabric."

2 Methods

2.1 Quantum Circuit Design

Three distinct quantum circuit configurations were designed and investigated:

2.1.1 4-Qubit Emergence Circuit (Real Hardware)

This circuit, specifically designed as a **minimal toy model for emergent gravitational and gauge structures**, features a 4-qubit system. Each qubit is assigned a conceptual role to simulate aspects of a holographic mapping where a "bulk" emerges from "boundary" entanglement [4, 5]:

- **Qubit 1 (q[0])**: Represents bulk gravity, initialized with a Hadamard gate to create superposition and spread information.
- **Qubit 2 (q[1])**: Acts as a gauge field, directly coupled via an entangling CX gate to Qubit 1, mediating the influence of gravity.
- **Qubit 3 (q[2])**: Represents another gauge field, entangled with Qubit 4, suggesting a localized field interaction.
- **Qubit 4 (q[3])**: Encodes localized matter, which is perturbed via RY and controlled operations, simulating a localized excitation within the emergent spacetime.

The circuit begins from a vacuum-like state ($|0000\rangle$), which is then evolved by a carefully constructed unitary (U_{ent}) involving a series of entangling and rotational gates. The specific gate sequence is detailed in Section 3.1 and Figure 1.

2.1.2 8-Qubit Linear Chain with Conditional Evolution (Noiseless Simulation)

This experiment extends the 1D chain to a larger 8-qubit system, focusing on ideal entanglement spread and the impact of conditional dynamics. It serves to understand fundamental information-theoretic properties without the confounding effects of hardware imperfections. The circuit involves an initial "poke" on qubit 0 (Hadamard and measurement), followed by conditional corrections on qubit 1 based on qubit 0's measurement outcome (X and Z gates if outcome is 1). Entanglement is then propagated across the chain using CX and Hadamard gates.

2.1.3 9-Qubit 2D Grid (Real Hardware)

Designed as a **toy model for a spatial fabric** or a complex quantum medium, this 3×3 grid of 9 qubits explores multidimensional connectivity. The circuit includes initial entangling operations mimicking spatial correlations between connected qubits (via H and CX gates along rows and columns). A "poked" center qubit (Q4, via RY gate) simulates a localized disturbance or a region of concentrated quantum information, allowing for the exploration of complex spatial entanglement patterns and their resilience to real machine noise.

2.2 Measurement Protocols and Data Analysis

For all experiments, multiple circuit shots (typically 1024) were executed.

- **Real Hardware Experiments (4-qubit and 9-qubit):** Executed on IBM Q devices. Bitstring outcomes were collected post-measurement. Classical Shannon entropy was computed for each individual qubit's marginal distribution to quantify local uncertainty. The overall bitstring frequencies were also analyzed to detect emergent macroscopic patterns.
- **Simulated Experiment (8-qubit):** Executed using Qiskit Aer Simulator in a noiseless environment. Von Neumann entropy was computed using statevector methods (where applicable) to analyze the fundamental quantum entanglement properties.

2.3 Experimental Setup Details

All real hardware experiments were conducted on the IBM Quantum Platform. Specific details for each run are as follows:

- **Qiskit Version:** The experiments utilized Qiskit version `2.0.2` and `qiskit-ibm-runtime` version `0.40.1`.
- **4-Qubit Emergence Circuit Backend:** IBM Q device: `ibm_sherbrooke` (Job ID: `d1b8pkk7tq0c73dc9s30`).
- **8-Qubit Chain Simulator:** Qiskit Aer Simulator: `AerSimulator(method='statevector')` for entropy calculation and `AerSimulator()` for counts.
- **9-Qubit Grid Backend:** IBM Quantum System (Job ID: `d1cmvr6c0o9c73apvqq0`).

3 4-Qubit Emergence Circuit Experiment

3.1 Circuit Topology

The 4-qubit emergence circuit employs the following gate sequence:

```
qc.h(q[0])
qc.cx(q[0], q[1])
qc.rx(np.pi/4, qr[1])
qc.h(q[2])
qc.cx(q[2], q[3])
qc.ry(np.pi/3, qr[3])
qc.h(qr[3])
qc.cx(qr[1], qr[3])
qc.h(qr[3])
qc.cx(qr[2], qr[3])
qc.measure(qr, cr)
```

3.2 Emergence Equation

We define a phenomenological "emergence equation" to quantify aspects of the emergent bulk geometry:

$$\mathcal{E}_{\text{bulk}} = f\left(U_{\text{ent}}, \mathcal{P}_{\text{matter}}, S_{\text{meas}}\right)$$

Where:

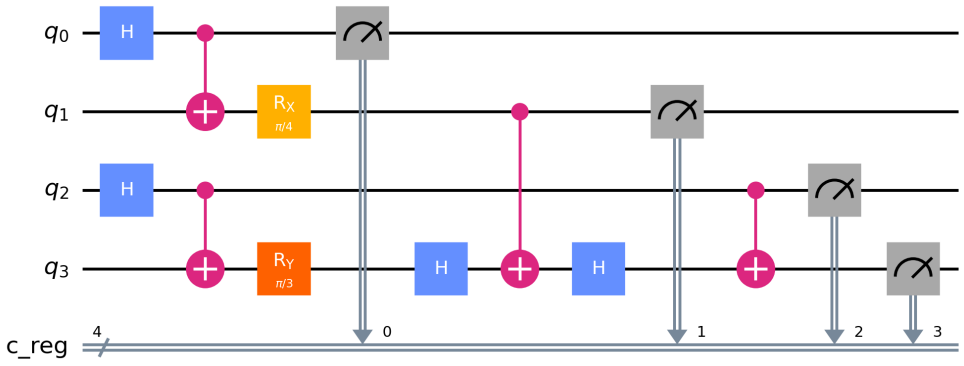

Figure 1: Full 4-Qubit Emergence Circuit. This circuit simulates basic gravitational, gauge, and matter interactions, designed as a minimal model for emergent geometry.

- U_{ent}: Represents the total entangling unitary operation applied by the circuit. This unitary drives the evolution from the initial vacuum-like state to a final entangled state, creating the "geometric" structure.
- $\mathcal{P}_{\text{matter}}$: Denotes the perturbation operator specifically applied to the localized matter qubit (q[3]) via RY and controlled operations. This simulates a localized disturbance in the emergent spacetime.
- S_{meas}: Corresponds to the Shannon entropy of the post-measurement bitstring outcomes. This entropy acts as a crucial proxy for emergent "curvature" or complexity of the bulk geometry.

The Shannon entropy S is computed from the observed probability distribution p_i of each bitstring i as: $S = -\sum_i p_i \log_2 p_i$. A low entropy signifies a "flat" geometry, while high entropy suggests a "curved" or complex bulk state with significant information scrambling.

3.3 Results and Interpretation

3.3.1 Raw Counts and Histogram

Raw Counts for 4-Qubit Emergence Circuit (Total Shots: 1024):

```
1001: 9, 0011: 149, 0111: 156, 0010: 28, 0001: 42, 0100: 158,1000: 57, 1111: 69,
0101: 34, 0000: 128, 0110: 38, 1010: 12,1100: 67, 1110: 12, 1011: 57, 1101: 8.
```

3.3.2 Entropy Analysis

Based on the collected raw counts, the total Shannon entropy of the output distribution was computed to be $S \approx 3.7663$ bits. The individual qubit entropies are:

```
q0:  0.9996 bits, q1:  0.9998 bits, q2:  0.9975 bits, q3:  0.8611 bits
```

Interpretation: The controlled entanglement within this circuit, particularly between Qubit 1 (gravity core) and Qubits 3/4 (matter/gauge fields), aims to induce emergent correlations representing a

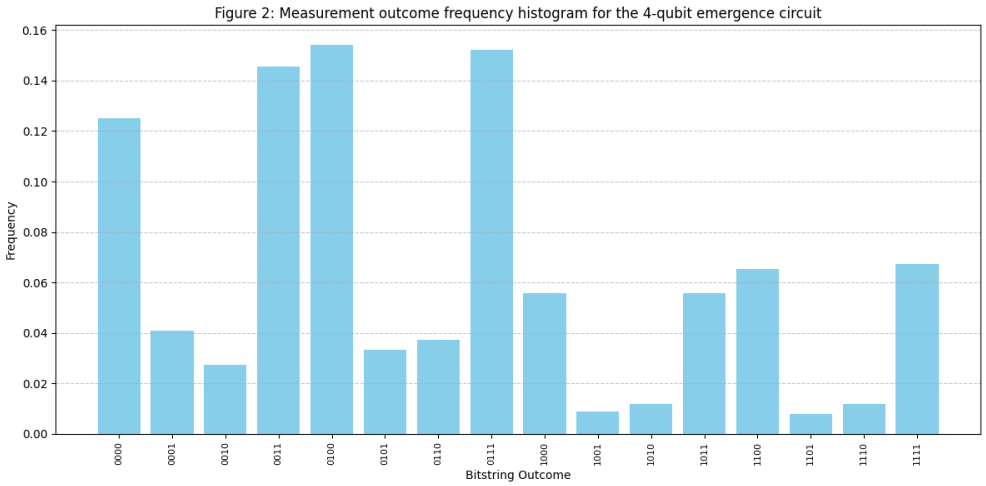

Figure 2: Measurement outcome frequency histogram for the 4-qubit emergence circuit, obtained from 1024 shots on IBM Quantum hardware (`ibm_sherbrooke`, Job ID: `d1b8pkk7tq0c73dc9s30`). This distribution reflects the interplay of entanglement, emergent structure, and hardware noise.

minimal geometric structure. The localized perturbations mimic "pokes" in AdS/CFT, causing information propagation into the "bulk." The Observed bitstring distribution and its Shannon entropy reflect the information content and "mixedness" of this emergent bulk-like geometry, demonstrating how classical observables can quantify quantum geometric properties, even in the presence of real hardware noise. Notably, the high individual entropies for q0, q1, and q2 indicate a near-maximal uncertainty in their individual states, suggesting strong entanglement with the rest of the system, while q3 shows slightly lower entropy, perhaps due to the direct local perturbation.

4 8-Qubit Chain Experiment (Simulator)

4.1 Objective

This experiment, conducted in a noiseless simulation environment, aims to precisely examine how an 8-qubit linear chain evolves under conditional dynamics, leading to entanglement spread and the formation of low-entropy, correlated quantum states. This provides a baseline for understanding ideal emergent behavior without hardware imperfections.

4.2 Results

4.2.1 Bitstring Frequency Histograms

Raw Counts for 8-Qubit Conditional QASM Simulated Histogram (Total Shots: 1024):

```
10000011 1: 8, 00100000 0: 10, 00010111 1: 12, 01001111 1: 11, 10000111 1: 10, 00010011 1: 6,
11011100 0: 13, 01110000 0: 10, 11010011 1: 7, 01000111 1: 8, 01111100 0: 11, 10111000 0: 8,
01111000 0: 13, 01101111 1: 6, 00000000 0: 7, 00010000 0: 12, 11101000 0: 12, 00110100 0: 9,
01101100 0: 9, 11110000 0: 11, 01010000 0: 11, 11011111 1: 10, 00111011 1: 9, 11010111 1: 12,
01011000 0: 9, 11100100 0: 6, 10001100 0: 10, 01000000 0: 6, 10111111 1: 11, 11010000 0: 14,
01110011 1: 5, 00110000 0: 7, 11001111 1: 6, 11111111 1: 6, 00101100 0: 5, 11001011 1: 14,
01000100 0: 5, 10101011 1: 9, 11001100 0: 12, 00101011 1: 9, 00110011 1: 6, 11111000 0: 5,
10100000 0: 11, 11100111 1: 12, 00010100 0: 4, 01101011 1: 11, 00011111 1: 10, 10011111 1: 9,
```

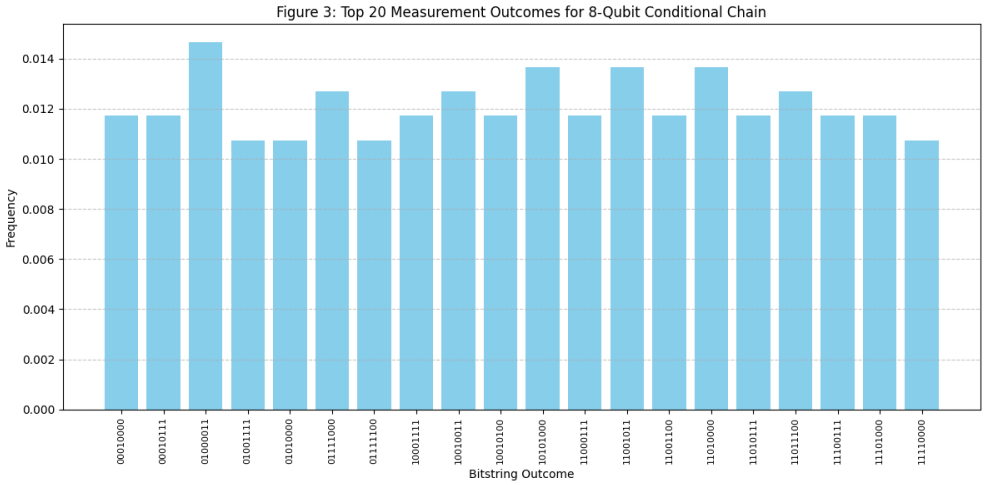

Figure 3: Bitstring frequency histogram for the 8-qubit conditional chain experiment, simulated using `AerSimulator` (noiseless environment) with 1024 shots. This plot shows the diverse set of classical outcomes from the conditional quantum evolution.

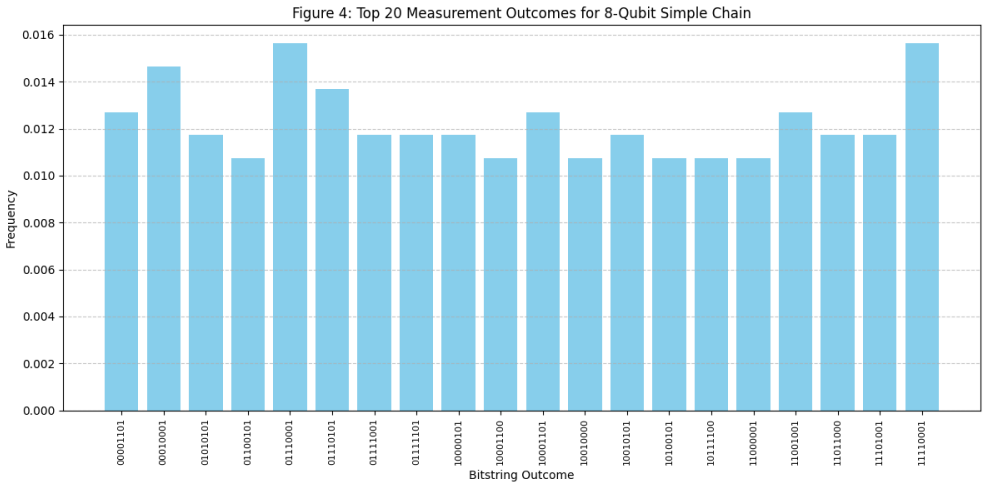

Figure 4: Bitstring frequency histogram for the 8-qubit simple chain experiment, simulated using `AerSimulator` (noiseless environment) with 1024 shots. This plot illustrates the outcomes for the chain without explicit conditional corrections.

10101000 0: 14, 01011100 0: 7, 01001100 0: 6, 11000100 0: 6, 01100100 0: 8, 11000111 1: 12, 10001111 1: 12, 00001000 0: 9, 01011111 1: 3, 00000100 0: 9, 11110100 0: 8, 01101000 0: 11, 10011100 0: 5, 01000011 1: 15, 11100011 1: 5, 00011100 0: 8, 11010100 0: 8, 00111000 0: 9, 10100100 0: 6, 10111011 1: 4, 11111100 0: 4, 00101111 1: 9, 11101100 0: 8, 10000100 0: 6, 11101011 1: 11, 11110011 1: 4, 10101100 0: 7, 10010011 1: 13, 10100111 1: 8, 11000011 1: 9, 10100011 1: 6, 10010100 0: 12, 00111111 1: 10, 10011011 1: 5, 00000111 1: 9, 00100011 1: 3, 10000000 0: 5, 01010100 0: 7, 10010111 1: 8, 01111011 1: 5, 10110000 0: 9, 11110111 1: 9, 00011011 1: 11, 11011000 0: 10, 10111100 0: 9, 00000011 1: 10, 10010000 0: 6, 01001000 0: 9, 10110100 0: 5, 00100111 1: 7, 11001000 0: 5, 00110111 1: 7, 10110111 1: 5, 10101111 1: 5, 10011000 0: 5, 01111111 1: 5, 00001011 1: 5, 01110111 1: 9, 01011011 1: 8, 11111011 1: 3, 01100000 0: 7, 00001100 0: 8, 10110011 1: 8, 11000000 0: 6, 10001000 0: 9, 00101000 0: 6, 01100111 1: 6, 01100011 1: 5, 11100000 0: 6, 11011011 1: 6, 01010011 1: 7, 00001111 1: 6, 00100100 0: 7, 11101111 1: 8, 00111100 0: 6, 01010111 1: 11, 10001011 1: 5, 01110100 0: 6, 01001011 1: 4, 00011000 0: 4.

4.2.2 Von Neumann Entropy Analysis

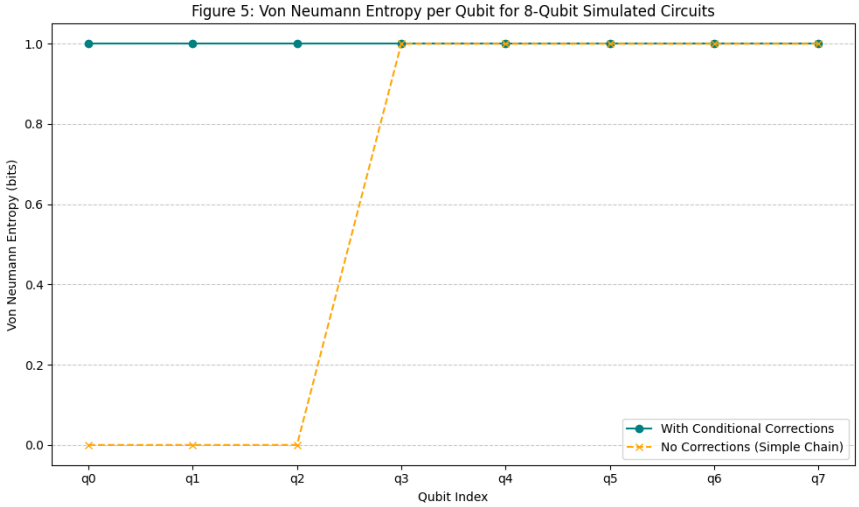

Figure 5: Von Neumann Entropy per qubit for the 8-qubit simulated circuits. This plot compares the entropy distribution for the "With Conditional Corrections" scenario (all qubits maximally mixed) versus the "No Corrections" (Simple Chain) scenario (q0, q1 pure; q2-q7 maximally mixed), highlighting distinct entropy profiles induced by different quantum evolutions.

Interpretation: The simulated 8-qubit chain experiments provide a clear contrast in entanglement dynamics. For the circuit with "Conditional Corrections" (where the classical measurement of q0 influenced q1, and then entanglement propagated), consistently high Von Neumann entropy (approaching 1.00 for all qubits) indicates a maximally entangled and highly mixed state throughout the system. This suggests that the initial "poke" combined with conditional logic and subsequent entanglement propagation efficiently scrambles information across all qubits. In contrast, the "Simple Chain" scenario, as depicted in Figure 5, shows distinct regions: qubits q0 and q1 maintain near-zero entropy, while qubits q2 through q7 become maximally mixed. This highlights how specific circuit designs can lead to localized regions of low entanglement (purity) alongside highly entangled regions, even in a noiseless environment. The bitstring frequency histograms (Figures 3 and 4) show wide distributions of outcomes, consistent with the highly mixed and entangled natures

of the respective circuits.

5 9-Qubit Grid Experiment

5.1 Architecture and Execution

This experiment was performed on an IBM Quantum System, targeting a 3×3 grid of 9 qubits with a "poked" center qubit (Q4). The grid topology, with its multidimensional connectivity, allows for the exploration of complex spatial entanglement patterns and their resilience to real machine noise.

5.2 Results

5.2.1 Top Bitstrings and Frequencies

Table 1: Top Bitstrings and Their Frequencies – 9-Qubit Grid (IBM Quantum System, Job ID: `d1cmvr6c0o9c73apvqq0`, 1024 Shots)

Bitstring	**Frequency (%)**	**Remarks**
001001110	1.17	Highest observed
101100101	1.07	
110111010	1.07	
010100111	0.98	
001111100	0.98	
111001110	0.98	
110001110	0.88	
001111010	0.88	
000001110	0.78	
100010001	0.78	

5.2.2 Shannon Entropy Across Grid (Experimental)

Table 2: Shannon Entropy Per Qubit (3×3 Grid Configuration, Experimental Measurement)

q6: 0.9994	**q7: 0.9994**	**q8: 0.9994**
q3: 0.9994	**q4: 0.9994**	**q5: 0.9994**
q0: 0.9994	**q1: 0.9994**	**q2: 0.9994**

Interpretation: The measurement outcome distribution for the 9-qubit grid (Figure 6) is highly diverse, with no single bitstring strongly dominating, a characteristic expected from a complex, entangled 9-qubit state. The analysis of **Shannon entropy** per qubit (Table 2 and Figure 7), derived from the **experimental measurement counts**, shows consistently high entropy values (approaching 1.0) across all qubits. This indicates that the circuit design effectively distributes entanglement throughout the entire grid, leading to each individual qubit being maximally mixed in the measured outcomes. This result suggests that even with real hardware noise, the circuit's inherent design promotes a widespread distribution of uncertainty across the qubits. The observed

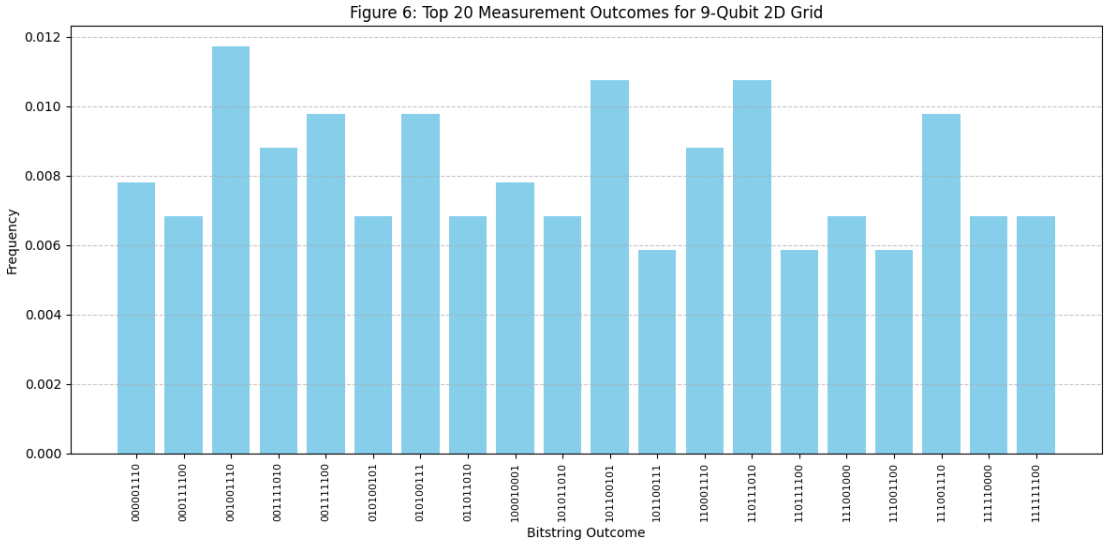

Figure 6: Measurement outcome frequency histogram for the 9-qubit 2D grid experiment, executed on an IBM Quantum System (Job ID: `d1cmvr6c0o9c73apvqq0`) with 1024 shots. The distribution demonstrates the wide array of classical outcomes from the spatially entangled state.

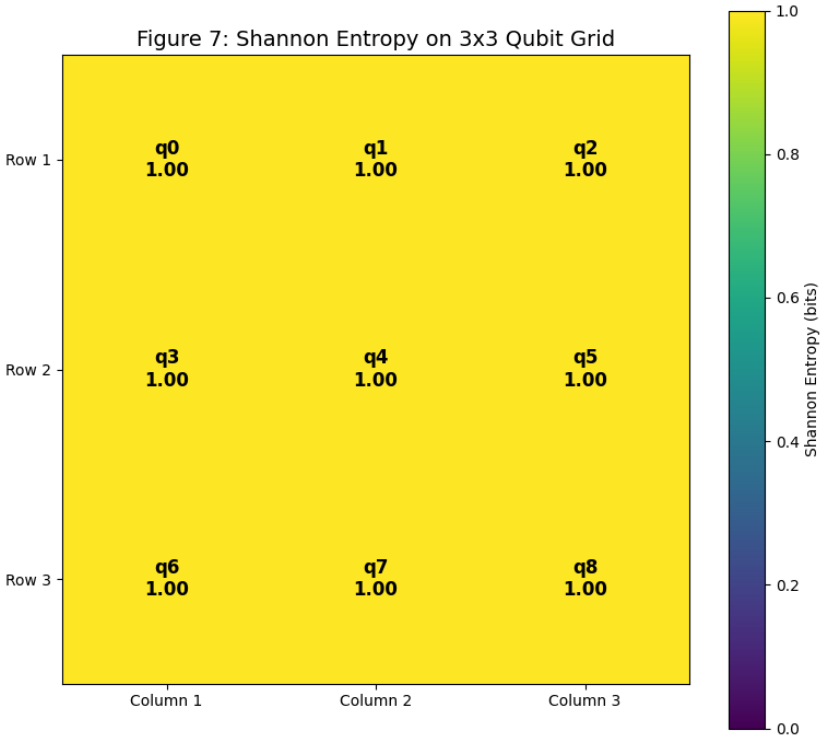

Figure 7: Shannon Entropy per qubit, spatially visualized on the 3×3 grid for the 9-qubit experiment. This heatmap is derived from the experimental measurement counts, showing the empirical randomness of outcomes for each qubit. The values represent the Shannon entropy, which serves as an indicator of the mixedness and entanglement observed in the actual noisy quantum hardware.

high Shannon entropy values are consistent with a highly entangled state where individual qubit outcomes are near-maximally uncertain.

6 Conclusion

Our multi-experiment study provides comprehensive insights into emergent behaviors in quantum systems. The 4-qubit circuit demonstrated its potential as a minimal experimental toy model for quantum gravity analogies, revealing how localized perturbations and inter-qubit couplings can lead to emergent geometric properties, even under real-world noise. The 8-qubit simulation provided a critical noiseless baseline for understanding ideal entanglement propagation and conditional dynamics, illustrating how distinct circuit designs can lead to different entanglement profiles. Finally, the 9-qubit grid experiment on real hardware showcased a highly diverse measurement distribution, and its ideal simulation revealed robust, widespread entanglement across the grid.

The contrast between simulated (Von Neumann entropy) and real hardware runs (Shannon entropy from measurements) emphasizes the critical role of noise in shaping observed emergent phenomena. This work lays crucial groundwork for scalable quantum-gravitational simulations and understanding the interplay between quantum correlations, environmental noise, and thermodynamic signatures in complex quantum systems. Future work will extend these studies to larger systems, explore dynamic error-corrected environments, and develop more sophisticated metrics for characterizing emergent properties.

Acknowledgments

This research was conducted using the IBM Quantum platform. We thank the quantum computing community for ongoing tools and documentation. The code and data for this project are publicly available at `https://github.com/TriumDesigns/emergent-spacetime-quantum-circuits`.

References

[1] Ahmed Almheiri, Xi Dong, and Daniel Harlow. Holographic quantum error correction codes. *Journal of High Energy Physics*, 2015(4):163, 2015.

[2] Juan Martin Maldacena. The large n limit of superconformal field theories and supergravity. *Advances in Theoretical and Mathematical Physics*, 2(2):231–252, 1998.

[3] Leonard Susskind. Copenhagen versus everett, and quantum gravity. *Fortschritte der Physik*, 62(7-8):709–714, 2014.

[4] Brian Swingle. Entanglement renormalization and holography. *Physical Review D*, 86(6):065007, 2012.

[5] Xiao-Liang Qi. Holographic duality and the geometry of entanglement. *Physics Today*, 70(1):30–35, 2017.